

Effects of humidity and temperature on quality factor of micro-beam resonators in atmospheric pressure and gas rarefaction

Nguyen Chi Cuong^{1*}, Trinh Xuan Thang¹, Lam Minh Thinh¹, Vuong Dinh Duy Phuc¹,
Phan Minh Truong², Truong Huu Ly¹, Ngo Vo Ke Thanh¹, Le Quoc Cuong¹

¹Research Laboratories of Saigon High-Tech Park,

Lot 13, N2 Street, Saigon High-Tech Park, Tan Phu Ward, District 9, Ho Chi Minh City, Vietnam

²Institute for Computational Science and Technology, SBI Building, Quang Trung Software City,
Tan Chanh Hiep Ward, District 12, Ho Chi Minh City, Vietnam

Received 10 March 2023; revised 1 June 2023; accepted 18 July 2023

Abstract:

At atmospheric pressure ($p=101325$ Pa), the effects of humidity and temperature on moist air become important when discussing the quality factor of micro-cantilever and micro-bridge resonators. The squeeze film damping (SFD) problem, the dominant damping source for micro-beam resonators, is modelled using the modified molecular gas lubrication (MMGL) equation with finite element modelling (FEM) in the eigenvalue problem. The MMGL equation is modified with the effective viscosity of moist air (μ_{eff}) to account for the effects of humidity and temperature. Other damping sources, such as thermoelastic damping (TED) and the support loss of micro-beam resonators, are also calculated. The quality factor of micro-beam resonators is then discussed over a wide range of temperatures and relative humidity levels at atmospheric pressure and gas rarefaction. The results show that the quality factor of micro-cantilever and micro-bridge resonators increases as both humidity and temperature rise in atmospheric pressure and gas rarefaction. Furthermore, the quality factor of a micro-bridge resonator with changes in humidity and temperature is significantly higher than that of a micro-cantilever resonator in atmospheric pressure and gas rarefaction.

Keywords: micro-beam resonators, quality factor, relative humidity, squeeze film damping, temperature.

Classification numbers: 2.1, 2.3

1. Introduction

Micro-beam resonators [1] are utilised in many Micro-Electro-Mechanical Systems (MEMS) sensor applications for environmental monitoring [e.g., temperature (T), humidity (RH), pollutant gases] [2, 3]. The advantages of temperature and humidity MEMS sensors based on MEMS technology include a wide detection range, rapid resonant response, and high precision. However, in moist air, the detection of temperature and water vapour plays a pivotal role in many MEMS sensor applications for environmental monitoring [4].

In MEMS resonators, the quality factor is the primary outcome when micro-beam resonators operate at atmospheric pressure. External SFD is one of the significant damping sources of MEMS resonators as

airflow is squeezed in the gap spacing between a micro-beam and its surrounding substrate [5]. In addition, TED [6-9] and support loss [10] are other damping sources for micro-beam resonators. For micro-beam structures of resonators, three kinds of damping sources - SFD, TED, and support loss - which are more dominant than other damping sources, have been considered to accurately evaluate the quality factor of micro-beam resonators [11]. At atmospheric pressure, the quality factor of micro-beam resonators is highly influenced by the effects of temperature (T) and humidity (RH) due to the increased viscous damping of moist air. Thus, the effects of temperature and relative humidity are crucial to discuss when aiming to improve the quality factor of micro-beam resonators since the transverse vibration of micro-beam resonators is significantly resisted by the SFD.

*Corresponding author: Email: cuong.nguyenchi@shtplabs.org

In gas rarefaction, atmospheric pressure ($p=101325$ Pa) is introduced into a narrow air gap spacing (h_0). Then, slip flow occurs on the micro-beam and substrate surfaces. Hence, the effect of gas rarefaction becomes significant on the dynamic performance of MEMS resonators, even at atmospheric pressure and ultra-thin gap spacing [11, 12]. To account for the effects of temperature and relative humidity in atmospheric pressure and gas rarefaction, the effective viscosity of moist air ($\mu_{eff}=\mu/Q_p$), which is defined as the ratio of the Poiseuille flow rate (Q_p) [13] and the dynamic viscosity (μ) [14] of moist air, modifying the MMGL equation for the SFD problem. As a result, the influences of temperature and relative humidity on the quality factor of micro-beam resonators can be addressed in both atmospheric pressure and gas rarefaction. Existing literature has examined the effects of temperature and relative humidity on the quality factors of MEMS resonators under atmospheric pressure [15-19]. Consequently, the quality factor of micro-cantilevers is heavily influenced by temperature and relative humidity in the atmospheric environment. However, the effects of temperature and relative humidity of moist air on the quality factor of micro-bridge resonators in atmospheric pressure and gas rarefaction have not yet been considered.

In this article, the impacts of temperature and relative humidity of moist air on the quality factor of micro-bridge resonators in atmospheric pressure and gas rarefaction for environmental monitoring are studied. The MMGL equation is solved using the effective viscosity (μ_{eff}) for the SFD issue to consider the effects of temperature and relative humidity across a range of pressures, from atmospheric to gas rarefaction. Previous studies have only addressed the temperature and relative humidity concerning the resonant frequency and quality factor of micro-cantilevers [18, 19] in atmospheric pressure. However, the micro-bridge structure has not been explored and discussed to date. In this research, the quality factor of the micro-bridge resonator will be discussed and compared to enhance the quality factors of MEMS resonators in atmospheric pressure and gas rarefaction. The objective of this study is to examine the effects of temperature and relative humidity of moist air in order to optimise the quality factors of MEMS resonators based on the micro-bridge structure for environmental monitoring in both atmospheric pressure and gas rarefaction.

2. Materials and methods

2.1. The modified molecular gas lubrication equation for air damping of micro-beam resonators

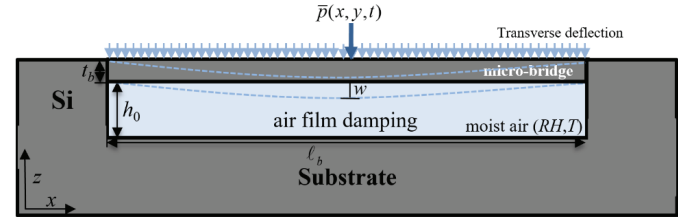


Fig. 1. Transverse vibration of micro-beam or micro-bridge resonators under air film damping.

In Fig. 1, the micro-bridge structure is used to discuss the effects of temperature and relative humidity on the quality factor of MEMS resonators in atmospheric pressure and gas rarefaction. In a moist air environment, the transverse motion of micro-beam resonators is resisted by the air film damping with a certain gas film pressure ($\bar{p}(x, y, t)$). The Poiseuille flow rate (Q_p) occurs in an ultra-thin gap spacing (h_0). In this instance, an isothermal air squeeze film is assumed for all the edges of the rectangular micro-bridge. The micro-beam temperature is assumed to be the same as the ambient temperature ($T=T_0$). A new MMGL equation [11] is utilised to model the SFD problem in order to obtain the pressure variations of the gas film as:

$$\frac{\partial}{\partial x} \left(\frac{\rho h^3}{12\mu_{eff}(RH, T)} \frac{\partial p}{\partial x} \right) + \frac{\partial}{\partial y} \left(\frac{\rho h^3}{12\mu_{eff}(RH, T)} \frac{\partial p}{\partial y} \right) = \frac{\partial}{\partial t} (\rho h) \quad (1)$$

where RH is the water vapor relative humidity (%); p is the air pressure, ρ is the density of moist air; h is the air gap spacing; T is the ambient temperature ($^{\circ}C$).

The water vapor molar fraction of moist air [14] is expressed as:

$$x_v = \frac{n_v}{n_v + n_a} = \frac{p_v}{p} \quad (2)$$

where p_v is the water vapor partial pressure; p is the total pressure partial pressure; x_v is the water vapor mole fraction; n_v and n_a are the water vapor and dry air mole numbers, respectively.

The relative humidity (RH) of moist air [14] is given by:

$$RH = \frac{x_v}{x_{sv}} = \frac{p_v}{p_{sv}} \quad (3)$$

with

$$x_v = x_{sv} \times RH \quad (4)$$

where p_v is the water vapor partial pressure; p_{sv} is the water vapor saturated pressure at a given temperature; x_{sv} is the saturated water vapor molar fraction.

The water vapor molar fraction (x_v) can be calculated as:

$$x_v = f(p, T) \times \frac{p_v}{p} = f(p, T) \times RH \times \frac{p_{sv}}{p} \quad (5)$$

with the total pressure (p) of moist air is given by:

$$p = p_v + p_a \quad (6)$$

where p_a is the partial pressure of dry air.

The enhancement factors ($f(p, T)$) [20] are calculated by:

$$f(p, T) = \exp\left[\alpha \times \left(1 - \frac{p_{sv}}{p}\right) + \beta \times \left(\frac{p}{p_{sv}} - 1\right)\right] \quad (7)$$

with

$$\alpha = \sum_{i=1}^4 A_i \times T^{(i-1)} \quad (8)$$

and

$$\beta = \exp\left(\sum_{i=1}^4 B_i \times T^{(i-1)}\right) \quad (9)$$

where the numerical values of the coefficients in Eqs. (8) and (9) are: $A_1=3.53624 \times 10^4$, $A_2=2.93228 \times 10^{-5}$, $A_3=2.61474 \times 10^{-7}$, $A_4=8.57538 \times 10^{-9}$, $B_1=-10.7588$, $B_2=6.32529 \times 10^{-2}$, $B_3=-2.53591 \times 10^{-4}$, and $B_4=6.33784 \times 10^{-7}$, in the temperature range between 0 and 100°C.

The saturated vapor pressure (p_{sv}) [21] is expressed by

$$p_{sv} = 10^3 \times 0.1 \times 10^e \quad (10)$$

where

$$e = E_0 + E_1 \left(1 - \frac{273}{T+273}\right) - E_2 \log_{10} \left(\frac{T+273}{273}\right) + E_3 \left(1 - 10^{-8.2969 \times \left(\frac{T+273}{273} - 1\right)}\right) + E_4 \left(10^{4.76955 \times \left(1 - \frac{273}{T+273}\right)}\right)$$

and

$$E_0=0.78614, E_1=10.79574, E_2=5.028, E_3=1.50475 \times 10^{-4}, E_4=0.42873 \times 10^{-3}.$$

At atmospheric pressure, the dynamic viscosity of humid air (μ) [14] is calculated by:

$$\mu = \frac{\mu_a \times (1-x_v)}{[(1-x_v) + x_v \Phi_{av}]} + \frac{x_v \times \mu_v}{[x_v + (1-x_v) \times \Phi_{va}]} \quad (11)$$

where μ_a and μ_v are the dynamic viscosity of dry air and water vapor, respectively, as:

$$\mu_a = M_{A_0} + \sum_{i=1}^4 M_{A_i} (T + 273)^i \quad (12)$$

$$\mu_v = M_{V_0} + M_{V_1} T \quad (13)$$

and

$$M_{A_0}=-9.8601 \times 10^{-7}, M_{A_1}=9.08012 \times 10^{-8}, M_{A_2}=-1.1764 \times 10^{-10}, M_{A_3}=1.2350 \times 10^{-13}, M_{A_4}=-5.797 \times 10^{-17}, M_{V_0}=8.058 \times 10^{-6}, \text{ and } M_{V_1}=4.0005 \times 10^{-8}$$

Also, Φ_{av} and Φ_{va} are calculated by

$$\Phi_{av} = \frac{\sqrt{2}}{4} \left(1 + \frac{M_a}{M_v}\right)^{-0.5} \times \left[1 + \left(\frac{\mu_a}{\mu_v}\right)^{0.5} \times \left(\frac{M_v}{M_a}\right)^{0.25}\right]^2 \quad (14)$$

$$\Phi_{va} = \frac{\sqrt{2}}{4} \left(1 + \frac{M_v}{M_a}\right)^{-0.5} \times \left[1 + \left(\frac{\mu_v}{\mu_a}\right)^{0.5} \times \left(\frac{M_a}{M_v}\right)^{0.25}\right]^2 \quad (15)$$

where Φ_{av} and Φ_{va} are interaction factors for calculating μ_a and μ_v , respectively; M_{A_i} and M_{V_i} are interpolation constants for the dynamic viscosity of dry air and water vapor, respectively; M_a and M_v are the dry air and water vapor molar mass, respectively.

For the effect of gas rarefaction, the Poiseuille flow rate $Q_p(D)$ [13] is derived for arbitrary inverse Knudsen number (D) with the accommodation coefficients of two surfaces ($\alpha_1=\alpha_2=1.0$) by:

$$Q_p(D) = 1 + 3\sqrt{\pi} \times a \times D^{-1} + 6b \times D^c \quad (16)$$

where $a=0.01807$, $b=1.35355$, $c=-1.17468$.

The inverse Knudsen number (D) is expressed by:

$$D = \frac{\sqrt{\pi}}{2Kn} = \frac{\sqrt{\pi}h}{2\lambda} \quad (17)$$

where h is the gap spacing.

The mean free path of gas is estimated from the kinetic theory of gases [22] is expressed as:

$$\lambda = \frac{RT}{\sqrt{2}\pi \times N_a d^2 p} \quad (18)$$

where d is the gas molecular diameter; $R=8.314$ (J/mol) is the gas constant; $N_a=6.0221 \times 10^{23}$ is Avogadro's number.

From Eqs. (3), (7), and (18), the mean free path of moist air (λ) can be expressed by:

$$\lambda = \frac{\lambda_0 p_0' T}{p T_0'} = \frac{\lambda_0 p_0' T}{(p_a + RH \cdot p_{sv}) T_0'} \quad (19)$$

where $\lambda_0=66.5$ nm, $p_0'=101325$ Pa, $T_0'=300$ K are the reference gas mean free path, reference pressure, and reference temperature, respectively.

The effective viscosity (μ_{eff}) of moist air [11] is expressed by:

$$\mu_{eff} = \frac{\mu}{Q_p} \quad (20)$$

where $\mu_{eff}(RH, T)$ can be used to consider the effects of temperature and relative humidity in atmospheric pressure and gas rarefaction.

2.2. The linear transverse vibration equation for micro-beam resonators

Under small displacement (w), the linear transverse vibration equation of a micro-beam in Fig. 1 governs the transverse displacement [23], which is expressed as:

$$D_p \left(\frac{\partial^4 w}{\partial x^4} + 2 \frac{\partial^4 w}{\partial x^2 \partial y^2} + \frac{\partial^4 w}{\partial y^4} \right) + \rho_m t_b \frac{\partial^2 w}{\partial t^2} = -\bar{p}(x, y, t) \quad (21)$$

where $D_p (=Et_b^3/12(1 - \nu^2))$ is the rigidity of the material; E is Young's modulus; ν is the Poisson's ratio; t_b is the structural thickness; $\bar{p}(x, y, t)$ is the gas pressure variation; $w(x, y, t)$ is the transverse displacement at positions along the structure (x, y) over time (t); ρ_m is the density of the material.

For a micro-cantilever beam [18, 19], single-clamped boundary conditions are used at one edge of the cantilever ($x=0$):

$$w(0, y, t) = 0 \quad (22)$$

$$\frac{\partial w(0, y, t)}{\partial x} = 0 \quad (23)$$

and three free boundaries are used at the other edges of the cantilever ($x=l_b, y=0, \text{ and } y=w_b$):

$$\frac{\partial^2 w(\ell_b, y, t)}{\partial x^2} = \frac{\partial^3 w(\ell_b, y, t)}{\partial x^3} = 0 \quad (24)$$

$$\frac{\partial^2 w(x, 0, t)}{\partial y^2} = \frac{\partial^3 w(x, 0, t)}{\partial y^3} = 0 \quad (25)$$

$$\frac{\partial^2 w(x, w_b, t)}{\partial y^2} = \frac{\partial^3 w(x, w_b, t)}{\partial y^3} = 0 \quad (26)$$

For a micro-bridge, the two double-clamped boundary conditions are set at two edges of the micro-bridge ($x=0$) and ($x=l_b$):

$$(0, y, t) = w(\ell_b, y, t) = 0 \quad (27)$$

$$\frac{\partial w(0, y, t)}{\partial x} = \frac{\partial w(\ell_b, y, t)}{\partial x} = 0 \quad (28)$$

and two free-edge conditions at other edges of the micro-bridge ($y=0, \text{ and } y=w_b$):

$$\frac{\partial^2 w(x, 0, t)}{\partial y^2} = \frac{\partial^3 w(x, 0, t)}{\partial y^3} = 0 \quad (29)$$

$$\frac{\partial^2 w(x, w_b, t)}{\partial y^2} = \frac{\partial^3 w(x, w_b, t)}{\partial y^3} = 0 \quad (30)$$

2.3. Quality factors of micro-beam resonators

In the eigen-value problem, the quality factor of the MEMS resonators in the SFD problem is numerically estimated by obtaining the eigenvalue ($\bar{\lambda} = \delta + i\omega$). Then,

the quality factor for the SFD problem (Q_{SFD}) [14] can be calculated as the ratio between the natural frequency (ω_0) ($Im|\bar{\lambda}|$) and the damping factor (δ) ($Re|\bar{\lambda}|$) by:

$$Q_{SFD} = \left| \frac{Im(\bar{\lambda})}{2 Re(\bar{\lambda})} \right| = \frac{\omega_0}{2\delta} \quad (31)$$

where $\bar{\lambda}(= \delta + i\omega)$ is the complex eigenvalue.

In micro-beam resonators, the total quality factor (Q_T) can be evaluated by the quality factor of the main damping sources of the SFD (Q_{SFD}), TED (Q_{TED}), and the support loss (Q_{sup}). Therefore, the total quality factor (Q_T) of the micro-cantilever and bridge beam resonators are calculated as:

$$\frac{1}{Q_T} = \frac{1}{Q_{SFD}} + \frac{1}{Q_{TED}} + \frac{1}{Q_{sup}} \quad (32)$$

where the basic operating conditions are listed in Table 1. Q_{TED} is calculated by C. Zener's models [6, 7] (Eq. (14) in [7]) in Table 2. Q_{sup} is also calculated by Z. Hao, et al. (2003) [10] (Eq. (18) in Table 3).

Table 1. Basic geometric and operating conditions of MEMS resonators.

Symbol	Description	Values
l_b	Length of beam	250 μm
w_b	Width of beam	10 μm
t_b	Thickness of beam	1 μm
E	Young's modulus of silicon	130 $\times 10^9$ Pa
ρ_m	Density of silicon	2330 kg/m ³
ν	Poisson's ratio of silicon	0.28
α_m	Thermal expansion coefficient of silicon	2.6 $\times 10^{-6}$ 1/K
κ	Thermal conductivity of silicon	90 W/(m.K)
C_p	Specific heat capacity of silicon cantilever	700 J/(kg.K)
h_0	Basic gas film thickness	4 μm
T_0	Basic temperature	50°C
p	Ambient pressure of moist air	101325 Pa
T	Ambient temperature	0-100°C
RH	Relative humidity of moist air	0-100%

Table 2. The quality factor of thermoelastic damping (TED) (Q_{TED}) for micro-beam resonators in the 1st mode of vibration.





Resonators	Mode shape	(Hz)	Q_{TED} in FEM [24]	Q_{Zener} in Zener [6, 7]	% Error $ \frac{Q_{TED}-Q_{Zener}}{Q_{TED}} \times 100\%$
Cantilever		19,344	21,738,340	22,589,923	3.77
Bridge		123,539	3,283,491	3,491,068	5.94

Table 3. The quality factor of support loss (Q_{sup}) for micro-beam resonators in the 1st mode of vibration.

Resonators	Mode shape	f_n (Hz)	$C_{(F(n))}$	λ_T	λ_T/w_b	Q_{sup} [10]
Cantilever		19,344	2.081	0.241	24,133	32,515,625
Bridge		123,539	0.638	0.038	3,778	9,968,750

3. Results and discussion

3.1. Effective viscosity, $\mu_{eff}(RH, T)$

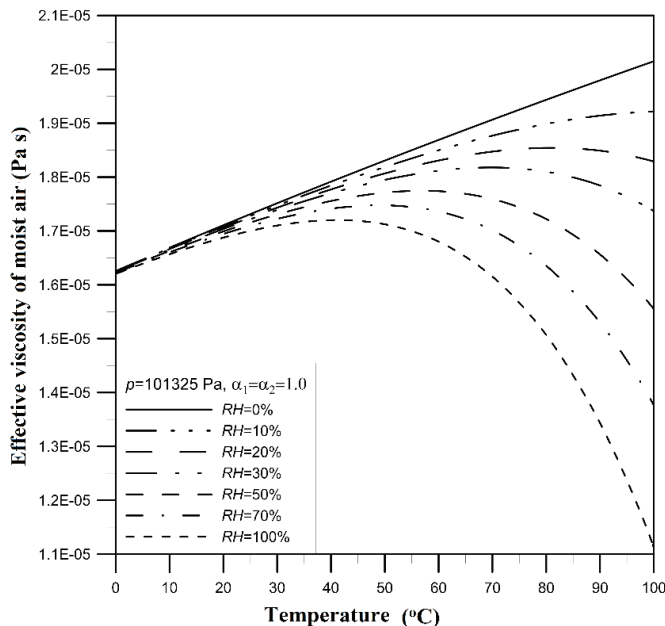


Fig. 2. Effective viscosity of moist air (μ_{eff}) versus temperature (T) for different relative humidity values (RH) at atmospheric pressure.

In Fig. 2, the effective viscosity of moist air (μ_{eff}), Eq. (20), in dry air linearly increases with T in the dry air ($RH=0\%$). Meanwhile, μ_{eff} of moist air decreases gradually as temperature and relative humidity increase. Therefore, we note that the effective viscosity (μ_{eff}) decreases more significantly as temperature and relative humidity increase.

3.2. Effects of temperature (T) and relative humidity (RH) on quality factors (Q_{SFD} , Q_T)

In Table 2, the results show that Q_{TED} and Q_{Zener} are very high because the TED is very small in the 1st mode of cantilever and bridge resonators. Moreover, Q_{TED} from the FEM (COMSOL Multiphysics) [24] and Q_{Zener} from the C. Zener's models [6, 7] are nearly identical with an error of less than 5.94%. Therefore, Q_{TED} in the FEM [24] can be accurately used to calculate the total quality factor (Q_T) of MEMS resonators.

In Table 3, the result showed that Q_{sup} is very high because the support loss is very small in the 1st mode of the resonators. Also, the results of Q_{sup} can be used to calculate the total quality factor (Q_T) of micro-beam resonators.

In Fig. 3, the obtained results of Q_{SFD} and Q_T of the micro-beam resonators are nearly identical over a wide range of temperature and humidity values at atmospheric pressure ($p=101325$ Pa). Therefore, Q_T can be calculated by the main contribution of Q_{SFD} because the SFD is the dominant damping source and the other damping sources (Q_{TED} , Q_{sup}) are negligible in the 1st mode of the resonator. Q_{SFD} and Q_T of dry air decreases as T increases. Q_{SFD} and Q_T of moist air increases as T increases while Q_{SFD} and Q_T of moist air increases as relative humidity (RH) increases from 0 to 100 % at atmospheric pressure. Then, Q_{SFD} and

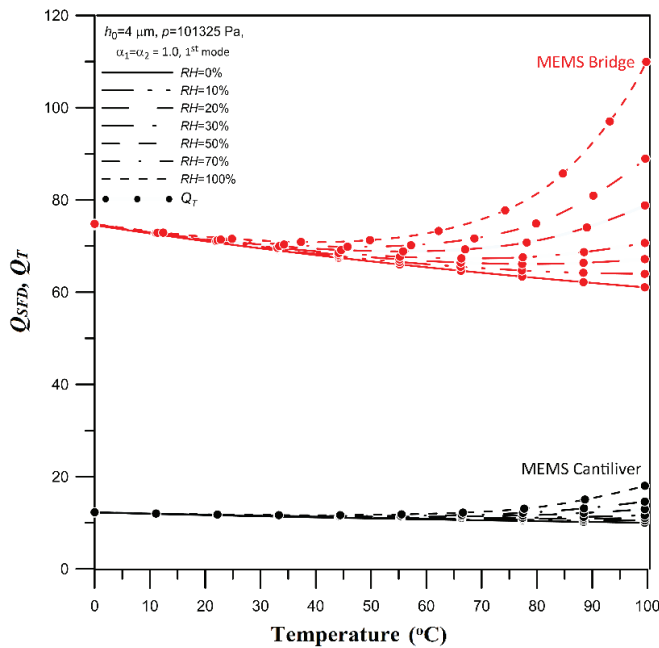


Fig. 3. The quality factor by SFD (Q_{SFD}) and total quality factor (Q_T) versus ambient temperature (T) for different relative humidity (RH) values in the 1st modes of MEMS cantilever and bridge beam resonators at atmospheric pressure ($p=101325$ Pa).

Q_T of moist air increases with temperature and relative humidity at $p=101325$ Pa. Also, Q_{SFD} and Q_T of the micro-cantilever with temperature and relative humidity is lower than that of the micro-bridge because of SFD influences on the cantilever being much stronger than that on the micro-bridge.

4. Conclusions

In these results, the quality factors of micro-beam resonators are numerically calculated by solving the MMGL equation, the equation of transverse vibration of the micro-beam, and their appropriate boundary conditions simultaneously using the FEM. The effective viscosity ($\mu_{eff}(RH, T)$) is utilised to modify the MMGL equation to consider the effects of temperature and relative humidity in atmospheric pressure and gas rarefaction. Some of the obtained results are shown as follows: (a) The quality factor of micro-beam resonators increases as the temperature and relative humidity increase in atmospheric pressure and gas rarefaction; (b) The quality factor of the micro-bridge resonator with temperature and relative humidity is much higher than that of the micro-cantilever resonator.

These highlighted results can be utilised to design for a high-quality factor and a fast resonant response of MEMS resonators. In future work, the design and fabrication process of temperature and humidity sensors based on micro-bridge resonators can be addressed and fabricated using MEMS technologies for environmental monitoring.

CRedit author statement

Nguyen Chi Cuong: Supervision, Conceptualisation, Writing - Reviewing; Trinh Xuan Thang, Lam Minh Thinh, Vuong Dinh Duy Phuc, Phan Minh Truong, Truong Huu Ly, Ngo Vo Ke Thanh, Le Quoc Cuong: Reviewing and Editing.

ACKNOWLEDGEMENTS

This research was supported by the Ho Chi Minh City Department of Science and Technology of Vietnam, Contract number 12/2021/HD-QKHCN on 24th March 2021. Also, this research was supported by the annual projects of the Research Laboratories of Saigon High-Tech Park, Board of Management of Saigon High-Tech Park, Decision number 17/QD-KCNC on 1st February 2023 (Project number 1).

COMPETING INTERESTS

The authors declare that there is no conflict of interest regarding the publication of this article.

REFERENCES

- [1] L. Wei, X. Kuai, Y. Bao, et al. (2021), "The recent progress of MEMS/NEMS resonators", *Micromachines*, **12(6)**, DOI: 10.3390/mi12060724.
- [2] P. Wei, Z. Ning, S. Ye, et al. (2018), "Impact analysis of temperature and humidity conditions on electrochemical sensor response in ambient air quality monitoring", *Sensors*, **18(2)**, DOI: 10.3390/s18020059.
- [3] Y. Zou, J.D. Clark, A.A. May (2021), "A systematic investigation on the effects of temperature and relative humidity on the performance of eight low-cost particle sensors and devices", *J. Aerosol. Sci.*, **152**, DOI: 10.1016/j.jaerosci.2020.105715.
- [4] D. Zhao, Y. Wang, J. Shao, et al. (2021), "Temperature and humidity sensor based on MEMS technology", *AIP Advances*, **11(8)**, DOI: 10.1063/5.0053342.

- [5] H. Hosaka, K. Itao, S. Kuroda (1995), “Damping characteristics of beam-shaped micro-oscillators”, *Sensors and Actuators A: Physical*, **49(1-2)**, pp.87-95, DOI: 10.1016/0924-4247(95)01003-J.
- [6] C. Zener (1937), “Internal friction in solids I theory of internal friction in reeds”, *Phys. Rev.*, **52(3)**, pp.230-235.
- [7] C. Zener (1938), “Internal friction in solids II general theory of thermoelastic internal friction”, *Phys. Rev.*, **53(1)**, pp.90-99.
- [8] Y. Fu, L. Li, Y. Hu (2019), “Enlarging quality factor in microbeam resonators by topology optimization”, *Journal of Thermal Stresses*, **42(3)**, pp.341-360, DOI: 10.1080/01495739.2018.1489744.
- [9] Y. Fu, L. Li, H. Chen, et al. (2022), “Rational design of thermoelastic damping in microresonators with phase-lagging heat conduction law”, *Applied Mathematics and Mechanics*, **43**, pp.1675-1690, DOI: 10.1007/s10483-022-2914-5.
- [10] Z. Hao, A. Erbil, F. Ayazi (2003), “An analytical model for support loss in micromachined beam resonators with in-plane flexural vibrations”, *Sensor. Actuat. A-Phy.*, **109(1-2)**, pp.156-164, DOI: 10.1016/j.sna.2003.09.037.
- [11] C.C. Nguyen, W.L. Li (2017), “Effect of gas rarefaction on the quality factors of micro-beam resonators”, *Microsyst. Technol.*, **23(8)**, pp.3185-3199, DOI: 10.1007/s00542-016-3068-z.
- [12] A.K. Pandey, R. Pratap (2007), “Effect of flexural modes on squeeze film damping in MEMS cantilever resonators”, *J. Micromech. Microeng.*, **17(12)**, pp.2475-2484, DOI: 10.1088/0960-1317/17/12/013.
- [13] C.C. Hwang, R.F. Fung, R.F. Yang, et al. (1996), “A new modified Reynolds equation for ultrathin film gas lubrication”, *IEEE Trans. Magn.*, **32(2)**, pp.344-347, DOI: 10.1109/20.486518.
- [14] P.T. Tsilingiris (2008), “Thermophysical and transport properties of humid air at temperature range between 0 and 100°C”, *Energ. Convers. Manage.*, **49(5)**, pp.1098-1110, DOI: 10.1016/j.enconman.2007.09.015.
- [15] E. Hosseinian, P.O. Theillet, O.N. Pierron (2013), “Temperature and humidity effects on the quality factor of a silicon lateral rotary micro-resonator in atmospheric air”, *Sensors and Actuators A: Physical*, **189**, pp.380-389, DOI: 10.1016/j.sna.2012.09.020.
- [16] H. Hosseinzadegan, O.N. Pierron, E. Hosseinian (2014), “Accurate modeling of air shear damping of a silicon lateral rotary micro-resonator for MEMS environmental monitoring applications”, *Sensors and Actuators A: Physical*, **216**, pp.342-348, DOI: 10.1016/j.sna.2014.06.008.
- [17] M.T. Jan, F. Ahmad, N.H.B. Hamid, et al. (2016), “Experimental investigation of temperature and relative humidity effects on resonance frequency and quality factor of CMOS-MEMS paddle resonator”, *Microelectron. Reliab.*, **63**, pp.82-89, DOI: 10.1016/j.microrel.2016.05.007.
- [18] Q.C. Le, M.T. Phan, X.T. Trinh, et al. (2021), “Temperature and relative humidity dependence of quality factors of mems cantilever resonators in atmospheric pressure”, *Sensing and Imaging*, **22(36)**, pp.1-30, DOI: 10.1007/s11220-021-00359-x.
- [19] C.C. Nguyen, M.T. Phan, X.T. Trinh, et al. (2022), “Effects of temperature and relative humidity on resonant frequency of MEMS cantilever resonators under atmospheric pressure”, *Vietnam Journal of Science and Technology*, **60(4)**, pp.724-736, DOI: 10.15625/2525-2518/16347.
- [20] L. Greenspan (1976), “Functional equations for the enhancement factors for CO₂-free moist air”, *J. Res. National. Bureau. Standards - A Phys. Chem.*, **80A(1)**, pp.41-44, DOI: 10.6028/jres.080A.007.
- [21] M.H. Hasan (2018), *Influence of Environmental Conditions on The Response of MEMS Resonators*, Master of Science Thesis, University of Nebraska-Lincoln, 114pp.
- [22] Z. Tan (2014), “Air pollution and greenhouse gases from basic concepts to engineering applications for air emission control”, *Green Energy and Technology*, Springer, DOI: 10.1007/978-981-287-212-8.
- [23] A.W. Leissa (1969), *Vibration of Plates*, NASA Technical Reports Server, 362pp.
- [24] COMSOL Multiphysics (2022), *Thermoelastic Damping in a MEMS Resonator*, <https://www.comsol.com/model/thermoelastic-damping-in-a-mems-resonator-1439>, accessed 24 November 2022.